$$\sum_{n=0}^{\infty} \tau^n \frac{d^n \mathbf{F}(t)}{dt^n} = \sum_{n=0}^{\infty} \left( \frac{1}{n!} \int_0^{\infty} s^n e^{-s}\, ds \right) \tau^n \frac{d^n \mathbf{F}(t)}{dt^n}$$
$$= \int_0^{\infty} e^{-s} \left( \sum_{n=0}^{\infty} \frac{(\tau s)^n}{n!} \frac{d^n \mathbf{F}(t)}{dt^n} \right) ds$$
$$= \int_0^{\infty} e^{-s} \mathbf{F}(t + \tau s) ds. \tag{9}$$

Nevertheless, we have seen that the two forms make different predictions when the force is suddenly turned on. What we have here is one of those instances for which the physicist must exercise some care with his mathematics. The calculation in (9) indicates that, when the future value of the force is expressible in terms of the force and its derivatives at time $t$,

$$\mathbf{F}(t + \tau s) = \sum_{n=0}^{\infty} \frac{(\tau s)^n}{n!} \frac{d^n \mathbf{F}(t)}{dt^n}, \tag{10}$$

then equations (4) and (7) are equivalent [actually uniform convergence of the integral in (9) is also required, but this is not the important point]. This being the case, it clearly makes no difference which equation is used for the calculation of numerical results, but (7) has the advantage of being manifestly causal, whereas (4) appears to violate causality. The violation is only apparent, however, because, in this case, the past and present force determine the future force completely. On the other hand, when the future force is not determined by the force and its derivatives at time $t$, then (4) and (7) are not equivalent, and one must decide which to adopt as the equation of motion for a charged particle. It is in this case that (4) truly violates the principle of causality, since the future force is quite independent of the past and present force.

An astute referee pointed out that, for the force (5), the equation of motion (7) is not totally free from difficulties because this force and all its derivatives are undefined at $t = 0$. To see more clearly the effect of the sudden change in the force, we write (5) as

$$\mathbf{F}(t) = \mathbf{F}_0 \int_{-\infty}^{t} \delta(t')dt'. \tag{11}$$

The equation of motion (7) then assumes the form

$$m\ddot{\mathbf{r}} = \mathbf{F}(t) + \mathbf{F}_0 \sum_{n=1}^{\infty} \tau^n \frac{d^{n-1}\delta(t)}{dt^n}, \tag{12}$$

which is indeed undefined at $t = 0$. But this is not a serious difficulty because changes of physical quantities across the discontinuity of $\mathbf{F}(t)$ are well defined. For example, the change of momentum $\mathbf{P}(= m\dot{\mathbf{r}})$ as time crosses $t = 0$ is the integral of (12) from $t = -\epsilon$ to $t = \epsilon$ with $\epsilon \to 0$. The result, which derives entirely from the $n = 1$ term in (12), is that the momentum jumps at $t = 0$ by the amount

$$\Delta \mathbf{P} = \tau \mathbf{F}_0. \tag{13}$$

This sudden change of momentum equals the accumulated change during the preacceleration period of Eq. (6). Hence the integrated momentum change is the same for both equations. But again we must emphasize that in no case does Eq. (7) violate causality.

We would therefore urge adoption of Eq. (7) as the only equation of motion for a nonrelativistic charged particle that is in accord with both the law of inertia and the principle of causality. Its only shortcoming is that it is not a closed-form expression. However, this seems a small price to pay to avoid the paradoxical, if not contradictory, aspects of preacceleration.


[1] H. A. Lorentz, *The Theory of Electrons* (Dover, New York, 1952), 2nd ed.
[2] M. Abraham, Ann. Phys. **10**, 105 (1903).
[3] R. Haag, Z. Naturforsch. Teil A **10**, 752 (1955).
[4] For the relativistic formulation of the integrodifferential equation, see F. Rohrlich, *Classical Charged Particles* (Addison-Wesley, Reading, MA, 1965), Chap. 6.
[5] J. D. Jackson, *Classical Electrodynamics* (Wiley, New York, 1975), 2nd ed., Chap. 17.


# Swinging Atwood's Machine


Nicholas B. Tufillaro,[a] Tyler A. Abbott, and David J. Griffiths
*Department of Physics, Reed College, Portland, Oregon 97202*



(Received 24 January 1983; accepted for publication 18 November 1983)



We examine the motion of an Atwood's Machine in which one of the masses is allowed to swing in a plane. Computer studies reveal a rich variety of trajectories. The orbits are classified (bounded, periodic, singular, and terminating), and formulas for the critical mass ratios are developed. Perturbative techniques yield good approximations to the computer-generated trajectories. The model constitutes a simple example of a nonlinear dynamical system with two degrees of freedom.


## I. INTRODUCTION

The advent of electronic computers has brought renewed interest in the once-intractable study of nonlinear dynamical systems. Even the simplest models, such as a pendulum on an elastic string,[1] can yield motions of surprising variety and complexity. We examine here the case of an ordinary Atwood's Machine, in which however one of the weights is allowed to swing in a plane (Fig. 1). The pulleys are massless and frictionless, and the rope is mass-

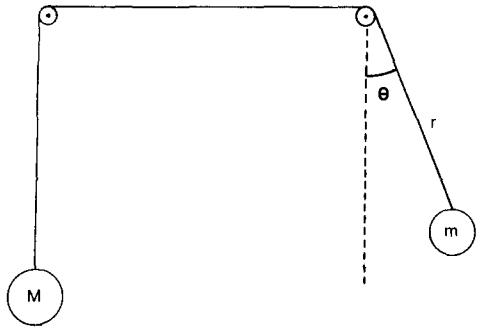


Fig. 1. Swinging Atwood's Machine.

less and inextensible. We assume the rope is long enough so that we need not worry about the counterweight ($M$) hitting the pulley; on the other hand, we shall allow the swinging mass ($m$) to rise above the horizontal line—and even to make complete loops around its pulley—provided the rope always remains taut.

It is not difficult to set up such a "Swinging Atwood's Machine" (SAM) in the laboratory. We used an air table mounted vertically to confine the swinging mass (an air puck) to the plane. The Ealing tables come with a hole through the center into which a pulley on a swivel can be inserted (Fig. 2). Friction is reduced by using an air pulley to support the counterweight. Although it is impossible, of course, to eliminate *all* dissipative forces, we have succeeded in demonstrating several of the motions described in this paper, using the laboratory model.

It might be supposed that SAM—like the simple Atwood's Machine—admits only runaway solutions (with the trivial exception of the equilibrium at $m = M$). But this is far from true; as we shall see, there is a rich variety of bounded and even periodic motions, which occur when $M$ exceeds $m$. Under appropriate conditions the centrifugal pseudoforce on the swinging mass balances the extra weight of the hanging mass, imparting to the system a kind of dynamical equilibrium with no counterpart in the simple Atwood's Machine.

In Sec. II we derive SAM's equations of motion, from which all the rest follows. The qualitative behavior of the trajectories is discussed in Sec. III; a number of computer solutions are presented, and some useful terminology is introduced. In the final sections we concentrate on two special classes of trajectories: "type A," whose limiting case is the simple pendulum (in Sec. IV), and "type B," which occur when $m$ is launched outward from the pulley and executes a symmetrical loop (in Sec. V). In each case we first determine the mass ratio and initial conditions which lead to motion of the specified type, and then develop a perturbation scheme for solving the equations of motion.

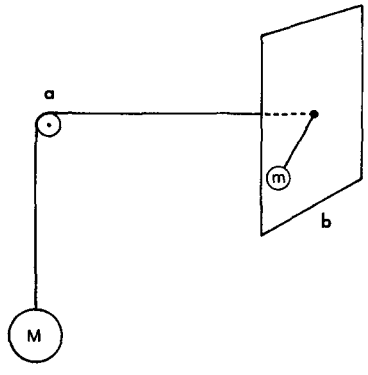


Fig. 2. Laboratory model of SAM. (a) Air pulley. (b) Air table, mounted vertically.

What we present here is certainly not an exhaustive study of the Swinging Atwood's Machine. We say nothing, for example, about unbounded motions (with $M \leqslant m$), and the trajectories we examine always begin from rest or from the origin. Our purpose is to call this delightful and intriguing problem to the attention of physics instructors, who may want to recommend it as a subject for independent projects by advanced undergraduates (as two of the authors were, when this work was undertaken). At the same time, we think the system should be of interest to applied mathematicians specializing in nonlinear dynamics, who have not, as far as we are able to determine, considered it.

## II. EQUATIONS OF MOTION

The Swinging Atwood's Machine has two degrees of freedom, which we shall take to be the $r$ and $\theta$ in Fig. 1. The kinetic energy for this system is

$$T = \tfrac{1}{2} M\dot{r}^2 + \tfrac{1}{2}m(\dot{r}^2 + r^2\dot{\theta}^2), \tag{1}$$

and the potential energy (apart from an arbitrary constant) is

$$V = gr(M - m\cos\theta), \tag{2}$$

where $g$ is the acceleration of gravity. The Lagrangian ($L = T - V$) is therefore

$$L = \tfrac{1}{2} M\dot{r}^2 + \tfrac{1}{2}m(\dot{r}^2 + r^2\dot{\theta}^2) + gr(m\cos\theta - M), \tag{3}$$

and the Euler–Lagrange equations $((d/dt)(\partial L/\partial \dot{q}_i) = \partial L/\partial q_i)$ yield

$$(m + M)\ddot{r} = mr\dot{\theta}^2 + g(m\cos\theta - M) \tag{4}$$

$$\frac{d}{dt}(mr^2\dot{\theta}) = -mgr\sin\theta. \tag{5}$$

Equation (4) represents Newton's Second Law in the radial direction, with the centrifugal term $mr\dot{\theta}^2$; Eq. (5) says that the rate of change of angular momentum is equal to the gravitational torque.

To simplify matters, define

$$\mu = M/m. \tag{6}$$

Then Eqs. (4) and (5) assume their final form:

$$(1 + \mu)\ddot{r} = r\dot{\theta}^2 + g(\cos\theta - \mu) \tag{7}$$

(which we shall call the "*radial equation*"), and

$$r\ddot{\theta} + 2\dot{r}\dot{\theta} + g\sin\theta = 0 \tag{8}$$

(the "*angular equation*"). SAM's motion is entirely determined by these two equations, together with appropriate starting conditions:

$$r(0) = r_0, \quad \theta(0) = \theta_0, \quad \dot{r}(0) = \dot{r}_0, \quad \dot{\theta}(0) = \dot{\theta}_0. \tag{9}$$

Because there is no dissipative force in this problem, the total energy

$$E = T + V = \tfrac{1}{2} M\dot{r}^2 + \tfrac{1}{2}m(\dot{r}^2 + r^2\dot{\theta}^2) + gr(M - m\cos\theta) \tag{10}$$

must be conserved—and it is easy to check [using Eqs. (4) and (5)] that $\dot{E} = 0$. The angular momentum of the swinging mass ($mr^2\dot{\theta}$) is *not* conserved, of course, because of the gravitational torque.

## III. QUALITATIVE BEHAVIOR

In this section we consider the qualitative behavior of the trajectory of the swinging mass. First, some terminology. We shall call the motion "bounded" if $r$ remains less than some fixed value for all time:

*Bounded trajectory*: $r(t) < r_{\max}$ for all $t \geqslant 0$.

[It turns out that *SAM's motion is bounded if* $M > m$. The proof is given in the Appendix. Although runaway (unbounded) solutions are of some interest, we shall confine our attention in this paper to bounded orbits, and hence the mass ratio $\mu$ will always be greater than 1.] The motion is "periodic" if after some time $\tau$ it repeats itself:

*Periodic trajectory*: $r(t+\tau) = r(t)$ and $\theta(t+\tau) = \theta(t)$, for all $t \geqslant 0$.

We call the trajectory "singular" if at some point $r$ goes to zero. The simplest way to set up a singular orbit is to fire $m$ outward from the origin, so that $r(0) = 0$. In fact, since the system is invariant under time reversal and time translation, we may as well arrange things so that our singular trajectories *always* begin this way:

*Singular trajectory*: $r(0) = 0$.

If $m$ subsequently collides with the pulley (never mind if it bounces off or passes through), $M$, which had been falling, must instantaneously reverse direction. So the tension in the rope is infinite, at such a moment, and for our purposes the motion terminates:

*Terminating singular trajectory*: $r(\tau) = r(0) = 0$, for some $\tau > 0$.

In some respects terminating singular trajectories are analogous to periodic (necessarily nonsingular) trajectories.

In Figs. 3–6 we display a number of computer-generated solutions to the equations of motion, to illustrate each kind of trajectory. The graphs in Fig. 3 are bounded and nonsingular; in each case $m$ is released from rest at $\theta_0 = 90°$ and allowed to run for several swings.[2] We surveyed the range from $\mu = 1$ to $\mu = 10$ in small increments, and picked out a sample of nine which give some indication of the variety available. Most of the curves have an ergodic appearance, and presumably would eventually fill in some region of the space. Others, however, are close to periodic. In the next study the computer was instructed to search the vicinity of each approximately periodic graph, using much finer mass increments. A sampling of the results is given in Fig. 4. (Each graph represents the superposition of many full cycles, so the width of the line is some measure of the departure from perfect periodicity.)

The third collection (Fig. 5) is a similar assortment of singular trajectories. This time $m$ is launched from the ori-

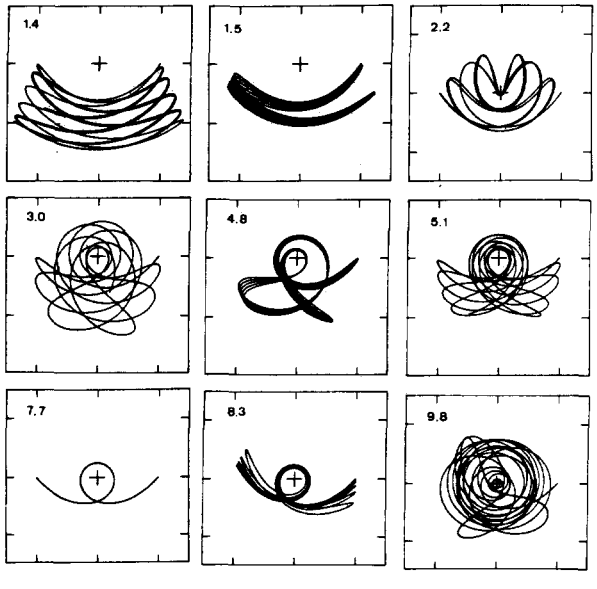


Fig. 3. Nonsingular trajectories. The mass ratio ($\mu$) is given in the upper left corner of each graph. The center ($r = 0$) is indicated with a cross. In each case the swinging bob was released from rest one unit to the right of the center.

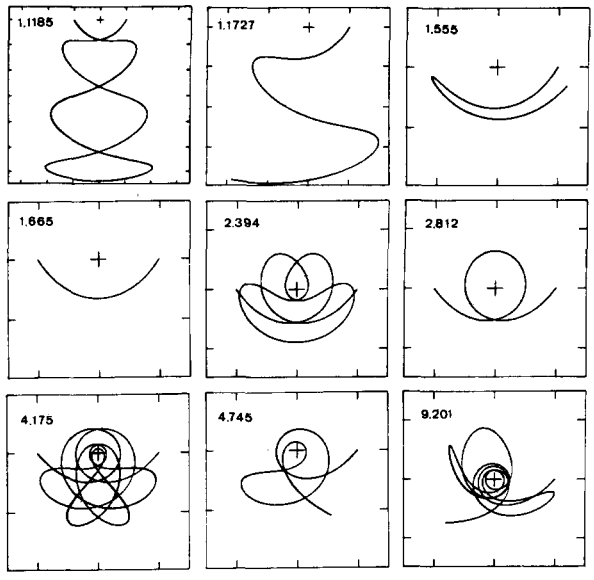


Fig. 4. Periodic trajectories. Mass ratio ($\mu$) is given in the upper left corner of each graph. Swinging mass again released from rest at $r_0 = 1$, $\theta_0 = 90°$.

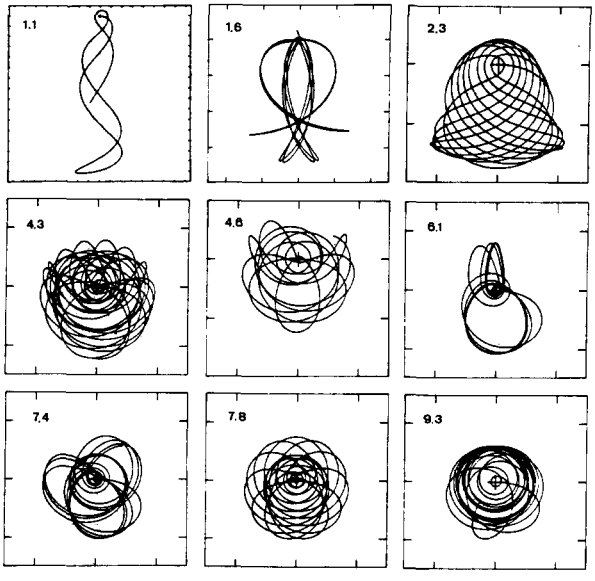


Fig. 5. Singular trajectories. Mass ratio ($\mu$) in upper left corner. The swinging mass was launched horizontally from the center, with an initial velocity $\dot{r}_0 = 4$.

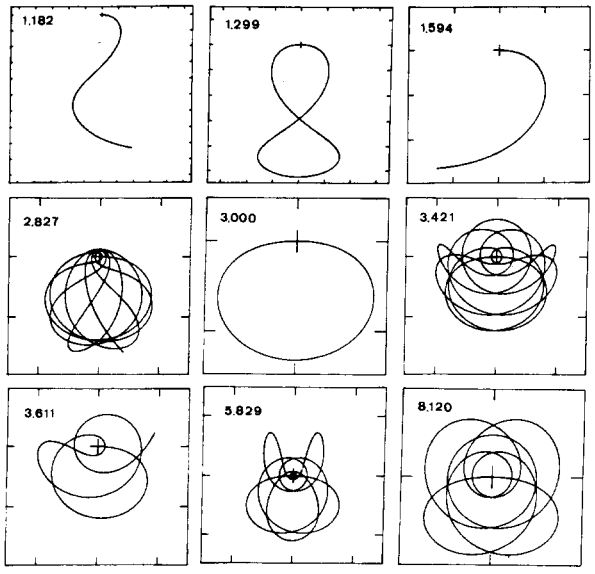


Fig. 6. Terminating trajectories. Mass ratio ($\mu$) in upper left corner. Swinging mass again launched from the center, with $\theta_0 = 90°$ and $\dot{r}_0 = 4$.

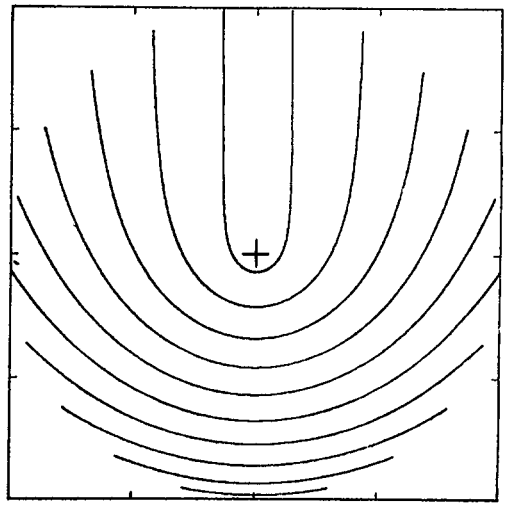

Fig. 7. Type A. The center is indicated by a cross. Swinging bob was released from rest at $r_0 = 2$, with $\theta_0$ ranging from 0.3–3.0 rad, in steps of 0.3 rad. Corresponding mass ratios are listed in Table I.

gin at an angle[2] of $\theta_0 = 90°$. As before, we surveyed the range from $\mu = 1$ to $\mu = 10$ in small increments, and picked out a representative sample. For most of the graphs there is no suggestion that $m$ will return to the origin. However, several of the graphs come *close* to terminating, and once again we had the computer search their neighborhoods using finer increments. The results are given in Fig. 6.

It is clear visually that there is a kind of natural hierarchy in the periodic and terminating trajectories. The cup-shaped "type A" solution at $\mu = 1.665$ is in some sense the "simplest" periodic orbit, while the oval-shaped "type B" solution at $\mu = 3.000$ is the simplest terminating trajectory. In the next two sections we shall study these two cases in greater detail.

## IV. TYPE A

The type A solution we found in Sec. III assumed an initial angle of 90°, but of course we can obtain similar trajectories for any $\theta_0$, provided we use the appropriate value of $\mu$.[3] Figure 7 displays a collection of computer-generated type A trajectories for $\theta_0$ ranging from 0.3–3.0 rad ($\mu$ ranges from 1.023 to 2.906). In each case the swinging mass was released from rest, at an initial distance $r_0 = 2$ (in arbitrary units).[4] *Question*: how do we determine the correct $\mu$, for a given starting angle $\theta_0$? It can, of course, be found numerically; the computer values are given in the first column of Table I, and plotted in Fig. 8. But we would like a *formula* for the function $\mu(\theta_0)$ which generates type A solutions.

It is easy to discover a small-angle approximation of $\mu(\theta_0)$, by observing that (a) for $\theta_0 \ll 1$, $r$ changes very little, so the trajectory is close to that of a simple pendulum, and (b) for any periodic motion the average tension in the rope must equal $Mg$. We obtain a condition on the mass ratio, then, by computing the average tension in a simple pendulum, and setting it equal to $Mg$. Now, the tension in a simple pendulum is

$$F = mr\dot{\theta}^2 + mg\cos\theta, \tag{11}$$

and for small angles the motion is simple harmonic:

$$\theta = \theta_0 \cos\omega t, \quad \text{where } \omega^2 = g/r. \tag{12}$$

The average tension is therefore

$$\langle F \rangle = mr\theta_0^2\omega^2\langle \sin^2 \omega t \rangle + mg\langle \cos(\theta_0 \cos\omega t) \rangle. \tag{13}$$

Table I. Mass ratios for type A. Computer-generated values are compared with the theoretical estimates given by Eqs. (15) and (17).

| Angle | Numerical | $1 + \theta_0^2/4$ | $J_0(\theta_0) + \theta_0^2/2$ |
|---|---|---|---|
| 0.1 | 1.002502 | 1.002500 | 1.002502 |
| 0.2 | 1.010027 | 1.010000 | 1.010025 |
| 0.3 | 1.022637 | 1.022500 | 1.022626 |
| 0.4 | 1.040427 | 1.040000 | 1.040398 |
| 0.5 | 1.063523 | 1.062500 | 1.063470 |
| 0.6 | 1.092068 | 1.090000 | 1.092005 |
| 0.7 | 1.126214 | 1.122500 | 1.126201 |
| 0.8 | 1.166103 | 1.160000 | 1.166287 |
| 0.9 | 1.211845 | 1.202500 | 1.212524 |
| 1.0 | 1.263503 | 1.250000 | 1.265198 |
| 1.1 | 1.321066 | 1.302500 | 1.324622 |
| 1.2 | 1.384436 | 1.360000 | 1.391133 |
| 1.3 | 1.453404 | 1.422500 | 1.465086 |
| 1.4 | 1.527647 | 1.490000 | 1.546855 |
| 1.5 | 1.606727 | 1.562500 | 1.636828 |
| 1.6 | 1.690092 | 1.640000 | 1.735402 |
| 1.7 | 1.777096 | 1.722500 | 1.842985 |
| 1.8 | 1.867017 | 1.810000 | 1.959986 |
| 1.9 | 1.959080 | 1.902500 | 2.086819 |
| 2.0 | 2.052481 | 2.000000 | 2.223891 |
| 2.1 | 2.146415 | 2.102500 | 2.371607 |
| 2.2 | 2.240097 | 2.210000 | 2.530362 |
| 2.3 | 2.332783 | 2.322500 | 2.700540 |
| 2.4 | 2.423785 | 2.440000 | 2.882508 |
| 2.5 | 2.512484 | 2.562500 | 3.076616 |
| 2.6 | 2.598347 | 2.690000 | 3.283195 |
| 2.7 | 2.680929 | 2.822500 | 3.502551 |
| 2.8 | 2.759885 | 2.960000 | 3.734964 |
| 2.9 | 2.834975 | 3.102500 | 3.980688 |
| 3.0 | 2.906076 | 3.250000 | 4.239948 |
| 3.1 | 2.973206 | 3.402500 | 4.512936 |

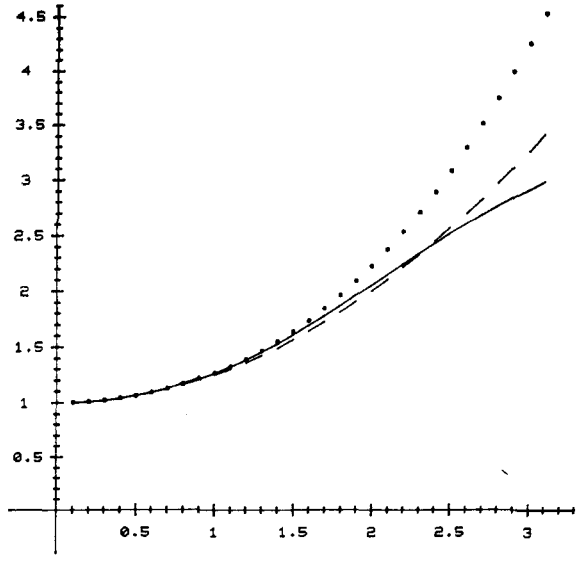


Fig. 8. Mass ratios for type A. The values in Table I are graphed. The vertical axis represents the mass ratio ($\mu$); the horizontal axis is starting angle ($\theta_0$), in radians. The solid line gives the computer results; the dashed line gives the theoretical estimate of Eq. (15); the dotted line is the theoretical estimate of Eq. (17).

The argument of $\cos(\theta_0 \cos \omega t)$ is small; keeping terms to order $\theta_0^2$ in the Taylor expansion gives

$$\langle F \rangle = mg\{\theta_0^2 \langle \sin^2 \omega t \rangle + 1 - (\theta_0^2/2)\langle \cos^2 \omega t \rangle\}$$
$$= mg(1 + \theta_0^2/4), \tag{14}$$

since $\langle \sin^2 \omega t \rangle = \langle \cos^2 \omega t \rangle = \frac{1}{2}$. Setting $\langle F \rangle = Mg$ yields the formula

$$\mu = 1 + \tfrac{1}{4}\theta_0^2. \tag{15}$$

Alternatively, we can evaluate the second term in Eq. (13) exactly—it is a Bessel function:

$$\langle \cos(\theta_0 \cos \omega t) \rangle = \frac{\omega}{2\pi} \int_0^{2\pi/\omega} \cos(\theta_0 \cos \omega t)\, dt = J_0(\theta_0), \tag{16}$$

giving

$$\mu = \theta_0^2/2 + J_0(\theta_0) \tag{17}$$

[which reduces to Eq. (15) when $J_0$ is expanded to second order]. These formulas are compared with the numerical data in Table I and Fig. 8. As expected, there is good agreement for small angles. Surprisingly, they remain fairly accurate even for relatively large angles. Equation (17) is distinctly better up to about 90°, beyond which neither formula is terribly good, though Eq. (15) is somewhat superior.

At the other extreme ($\theta_0$ close to 180°) the numerical results appear to be heading for $\mu = 3$, and this limiting value can be confirmed theoretically as follows. When $\theta_0 \approx 180°$, the swinging mass is dropped from a point almost directly above the pulley; it falls practically straight down, with the acceleration of gravity, until it is very close to the pulley, whereupon it executes a sudden hairpin turn around the pulley and flies straight up again on the other side. Most of the time the mass is essentially in free fall, but for a split second it is subject to a huge tension in the rope, as it reverses direction. Now, the point is that this sudden jerk must accomplish a precisely 360° turn—if $m$ is too heavy, it will not make the full turn, and if $m$ is too light it will execute a complete loop and then some. Our problem, then, is to analyze the motion during the bend in the hairpin, when the tension in the rope dominates the force of gravity, so that we may set $g = 0$ in the equations of motion:

$$(1 + \mu)\ddot{r} = r\dot{\theta}^2, \tag{18}$$

$$r\ddot{\theta} + 2\dot{r}\dot{\theta} = 0. \tag{19}$$

The angular equation says that $(d/dt)(r^2\dot{\theta}) = 0$, so $r^2\dot{\theta} = l$, a constant (in this régime angular momentum is conserved). Eliminating $\dot{\theta}$ from the radial equation, we have

$$(1 + \mu)\ddot{r} = l^2/r^3. \tag{20}$$

Letting $u = 1/r$, and eliminating $t$ in favor of $\theta$ [$\dot{r} = (dr/du)(du/d\theta)(d\theta/dt)$, etc.], we find

$$\frac{d^2u}{d\theta^2} = -\frac{1}{(1 + \mu)}u, \tag{21}$$

and the general solution is

$$u(\theta) = A \cos \kappa(\theta - \theta_1), \tag{22}$$

where

$$\kappa = 1/\sqrt{1 + \mu} \tag{23}$$

and $\theta_1$ is the angle of closest approach (where $u$ is a maxi-

Table II. Mass ratios for simple terminating orbits. For starting angles ($\theta_0$) in radians, computer-determined mass ratios are listed for the four simplest terminating trajectories. The top line gives the "magic mass" formula prediction [Eq. (36)].

| Angle | B1 | B2 | B3 | B4 |
|---|---|---|---|---|
| Magic | 3.000 | 1.500 | 1.250 | 1.154 |
| 0.1 | 3.000 | 1.500 | 1.250 | 1.154 |
| 0.2 | 3.000 | 1.501 | 1.250 | 1.154 |
| 0.3 | 3.000 | 1.502 | 1.251 | 1.155 |
| 0.4 | 3.000 | 1.505 | 1.252 | 1.155 |
| 0.5 | 3.000 | 1.507 | 1.254 | 1.156 |
| 0.6 | 3.000 | 1.511 | 1.255 | 1.157 |
| 0.7 | 3.000 | 1.515 | 1.258 | 1.157 |
| 0.8 | 3.000 | 1.520 | 1.260 | 1.158 |
| 0.9 | 3.000 | 1.525 | 1.263 | 1.161 |
| 1.0 | 3.000 | 1.532 | 1.266 | 1.163 |
| 1.1 | 3.000 | 1.539 | 1.270 | 1.166 |
| 1.2 | 3.000 | 1.548 | 1.275 | 1.168 |
| 1.3 | 3.000 | 1.558 | 1.280 | 1.171 |
| 1.4 | 3.000 | 1.570 | 1.286 | 1.175 |
| 1.5 | 3.000 | 1.583 | 1.293 | 1.179 |
| 1.6 | 3.000 | 1.598 | 1.301 | 1.182 |
| 1.7 | 3.000 | 1.616 | 1.310 | 1.188 |
| 1.8 | 3.000 | 1.637 | 1.321 | 1.194 |
| 1.9 | 3.000 | 1.661 | 1.334 | 1.201 |
| 2.0 | 3.000 | 1.690 | 1.349 | 1.209 |
| 2.1 | 3.000 | 1.725 | 1.367 | 1.218 |
| 2.2 | 3.000 | 1.767 | 1.390 | 1.229 |
| 2.3 | 3.000 | 1.819 | 1.418 | 1.250 |
| 2.4 | 3.000 | 1.883 | 1.453 | 1.259 |
| 2.5 | 3.000 | 1.965 | 1.500 | 1.279 |
| 2.6 | 3.000 | 2.071 | 1.564 | 1.305 |
| 2.7 | 3.000 | 2.208 | 1.656 | 1.338 |
| 2.8 | 3.000 | 2.381 | 1.804 | 1.383 |
| 2.9 | 3.000 | 2.582 | 2.056 | 1.446 |
| 3.0 | 3.000 | 2.780 | 2.474 | 1.536 |
| 3.1 | 3.000 | 2.944 | 2.879 | 1.654 |

mum). We want this to occur at the bottom of the swing, so $\theta_1 = 0$, and

$$r(\theta) = 1/A \cos \kappa\theta. \tag{24}$$

Now, for a perfect U-turn, $r \to \infty$ (for the first time) at $\pm\pi$, which means that $\kappa = \frac{1}{2}$, and therefore $\mu = 3$, *Q.E.D.* [By the same reasoning, the limiting mass ratio for a *loop*—$\mu = 2.812$ in Fig. 4—would be $\mu(\pi) = 15$.]

The equations of motion,

$$(1 + \mu)\ddot{r} = r\dot{\theta}^2 + g(\cos\theta - \mu), \tag{7}$$

$$r\ddot{\theta} + 2\dot{r}\dot{\theta} + g \sin\theta = 0, \tag{8}$$

can be solved, for the case of a type A trajectory, in the form of a perturbative expansion in powers of $\theta_0$ (which, it should be noted, is the largest value $\theta$ assumes):

*Zeroth order.* $\begin{cases} \text{radial equation:} & (1 + \mu)\ddot{r} = g(1 - \mu) \\ \text{angular equation:} & 0 = 0. \end{cases}$

The general solution to the radial equation, to this order, is

$$r(t) = A + Bt + \frac{1}{2} g\left(\frac{1 - \mu}{1 + \mu}\right) t^2.$$

The constants $A$ and $B$ are determined by the initial conditions:

$$\begin{cases} \dot{r}(0) = 0 \Rightarrow B = 0 \\ r(0) = r_0 \Rightarrow A = r_0, \end{cases}$$

and the mass ratio is fixed by requiring that the motion be bounded:

$$\text{bounded} \Rightarrow \mu = 1.$$

Thus to zeroth order we have

$$r(t) = r_0;\ \theta(t) \text{ undetermined; with } \mu = 1. \tag{25}$$

*First order.* $\begin{cases} \text{radial equation:} & (1 + \mu)\ddot{r} = g(1 - \mu) \\ \text{angular equation:} & r\ddot{\theta} + 2\dot{r}\dot{\theta} + g\theta = 0. \end{cases}$

The radial equation is unchanged from zeroth order, so the solution ($r(t) = r_0, \mu = 1$) carries over to first order. Putting this into the angular equation, we have

$$r_0\ddot{\theta} + g\theta = 0,$$

with the general solution

$$\theta(t) = A \cos\omega t + B \sin\omega t, \quad \omega = \sqrt{g/r_0}.$$

The constants $A$ and $B$ are determined by the initial conditions:

$$\begin{cases} \dot{\theta}(0) = 0 \Rightarrow B = 0 \\ \theta(0) = \theta_0 \Rightarrow A = \theta_0. \end{cases}$$

Thus to first order we have

$$r(t) = r_0;\ \theta(t) = \theta_0 \cos\omega t,$$

$$\text{with } \mu = 1 \text{ and } \omega = \sqrt{g/r_0}. \tag{26}$$

Not surprisingly, this is nothing but a simple pendulum.

*Second order.* $\begin{cases} \text{radial equation:} & (1 + \mu)\ddot{r} = r\dot{\theta}^2 + g(1 - \theta^2/2 - \mu) \\ \text{angular equation:} & r\ddot{\theta} + 2\dot{r}\dot{\theta} + g\theta = 0. \end{cases}$

The angular equation is unchanged from first order, so the solution ($\theta(t) = \theta_0 \cos\omega t$; $\omega = \sqrt{g/r_0}$) carries over to second order. Putting this into the radial equation, we find

$$(1 + \mu)\ddot{r} = r\theta_0^2\omega^2 \cos^2\omega t + g(1 - \mu - \tfrac{1}{2}\theta_0^2 \cos^2\omega t).$$

Now the first term on the right is already of second order, so it suffices to use $r = r_0$ in that position. Thus

$$\begin{aligned}(1 + \mu)\ddot{r} &= g[1 - \mu + \theta_0^2(\sin^2\omega t - \tfrac{1}{2}\cos^2\omega t)] \\ &= g[1 - \mu + (\theta_0^2/4)(1 - 3\cos 2\omega t)]. \end{aligned} \tag{27}$$

Notice that the swinging pendulum drives the radial motion at double the angular frequency. This is as it should be, since the centrifugal pseudoforce hits a maximum twice in each cycle. The general solution to Eq. (27) is

$$r(t) = A + Bt + \frac{g}{2(1 + \mu)}\left\{\left(1 - \mu + \frac{\theta_0^2}{4}\right) t^2 + \frac{3\theta_0^2}{8\omega^2}\cos 2\omega t\right\}$$

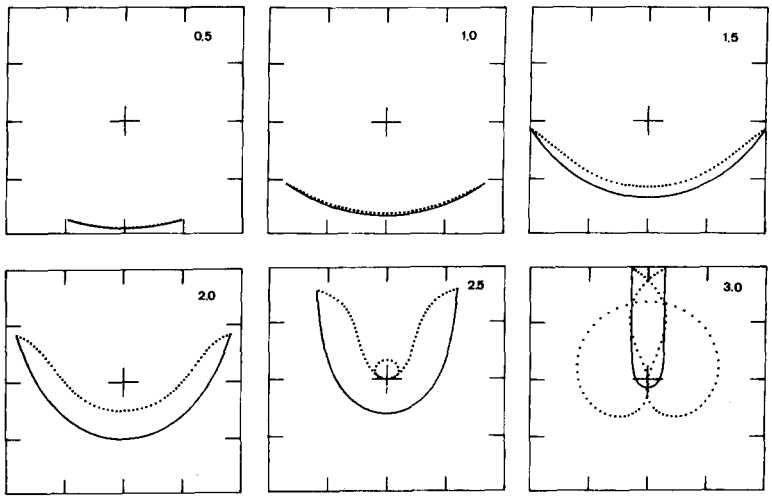


Fig. 9. Perturbative type A trajectories. These graphs compare the exact (computer-generated) type A solutions (solid lines) with the third-order perturbation theory (dotted lines), as given by Eqs. (29) and (30). In each case the swinging bob was released from rest at $r_0 = 2$; the starting angles ($\theta_0$) are given in the upper right corner, in radians.

and

$$\begin{cases} \dot{r}(0) = 0 \Rightarrow B = 0 \\ r(0) = r_0 \Rightarrow A = r_0 - \dfrac{g}{2(1+\mu)} \dfrac{3\theta_0^2}{8\omega^2} \end{cases};$$

bounded $\Rightarrow \mu = 1 + \theta_0^2/4$.

The latter neatly reproduces Eq. (15), and we conclude that, to second order,

$$r(t) = r_0(1 - \tfrac{3}{16}\theta_0^2 \sin^2 \omega t); \quad \theta(t) = \theta_0 \cos \omega t;$$

$$\text{with } \omega = \sqrt{g/r_0} \text{ and } \mu = 1 + \theta_0^2/4. \tag{28}$$

*Third order.* In the same way, the third-order calculation yields

$$r(t) = r_0(1 - \tfrac{3}{16}\theta_0^2 \sin^2 \bar{\omega} t),$$

$$\theta(t) = \theta_0 \cos \bar{\omega} t\,(1 + \tfrac{53}{384}\theta_0^2 \sin^2 \bar{\omega} t), \tag{29}$$

with

$$\bar{\omega} = \omega(1 + \tfrac{7}{128}\theta_0^2), \quad \omega = \sqrt{g/r_0}, \quad \text{and } \mu = 1 + \theta_0^2/4. \tag{30}$$

A comparison between the third-order perturbative approximation and computer-generated trajectories is given in Fig. 9. The approximation is very good for small angles; not surprisingly, there are noticeable discrepancies when $\theta_0$ exceeds 90°.

## V. TYPE B

In Sec. IV we analyzed type A solutions (the simplest *periodic* trajectories) as perturbations on the simple pendulum. In this section we study type B solutions (the simplest *terminating* trajectories) as perturbations on the simple Atwood's Machine. As before, we shall expand the equations of motion in powers of $\theta$, with a view to answering two questions: (i) for what mass ratios $\mu(\theta_0)$ do terminating trajectories occur, and (ii) what is the (approximate) shape of the orbit?

We consider, then, the case in which mass $m$ is fired outward from the origin, with an initial speed $v$, at an initial angle $\theta_0$.

*Zeroth order.* $\begin{cases} \text{radial equation:} & (1+\mu)\ddot{r} = g(1-\mu) \\ \text{angular equation:} & 0 = 0. \end{cases}$

General solution:

$$r(t) = A + Bt + \frac{1}{2} g\left(\frac{1-\mu}{1+\mu}\right) t^2.$$

Initial conditions:

$$\begin{cases} r(0) = 0 \Rightarrow A = 0 \\ \dot{r}(0) = v \Rightarrow B = v. \end{cases}$$

To zeroth order, then,

$$r(t) = vt - \frac{1}{2} a t^2, \quad \text{where } a = \left(\frac{\mu - 1}{\mu + 1}\right) g. \tag{31}$$

This is, of course, a simple Atwood's Machine, in which the lighter mass is thrown straight down, and returns to the pulley after a time

$$\tau = 2v/a, \tag{32}$$

at which point the motion terminates.

*First order.* $\begin{cases} \text{radial equation:} & (1+\mu)\ddot{r} = g(1-\mu) \\ \text{angular equation:} & r\ddot{\theta} + 2\dot{r}\dot{\theta} + g\theta = 0. \end{cases}$

The radial equation is unchanged; putting the zeroth-order solution for $r(t)$ into the angular equation, we have

$$(vt - \tfrac{1}{2}at^2)\ddot{\theta} + 2(v - at)\dot{\theta} + g\theta = 0. \tag{33}$$

Assuming the solution admits a Taylor expansion, we may write

$$\theta(t) = \sum_{n=0}^{\infty} b_n t^n, \tag{34}$$

and, upon substitution into Eq. (33), obtain the following recursion formula for the coefficients:

$$b_{n+1} = b_n \left(\frac{(a/2)n(n+3) - g}{v(n+1)(n+2)}\right), \quad n = 0,1,2,3,\ldots. \tag{35}$$

If the sequence continues indefinitely, then for large $n$,

$$b_{n+1} \sim b_n(a/2v)$$

and we have

$$\theta(t) \sim \sum_{n=0}^{\infty} \left(\frac{at}{2v}\right)^n = \frac{1}{1 - (at/2v)},$$

which blows up as $t \to \tau$. The solutions we seek, however, maintain a small angle throughout the motion; evidently they occur only when the sequence of $b_n$'s truncates at some maximal $n$:

$$b_{N+1} = 0 \Rightarrow (a/2)N(N+3) = g.$$

In this case $\theta(t)$ is a polynominal[5] of degree $N$. Using Eq. (31) to eliminate $a$, we find

$$\mu = \frac{(N+1)(N+2)}{N^2 + 3N - 2}, \quad N = 1,2,3,\ldots. \tag{36}$$

We shall call this the "magic mass" formula; it tells us the mass ratios which lead to terminating singular trajectories, in the limit of small angles. Figure 10 displays computer-generated solutions to the equations of motion for the first nine such terminating orbits, using $\theta_0 = 0.5$ rad.

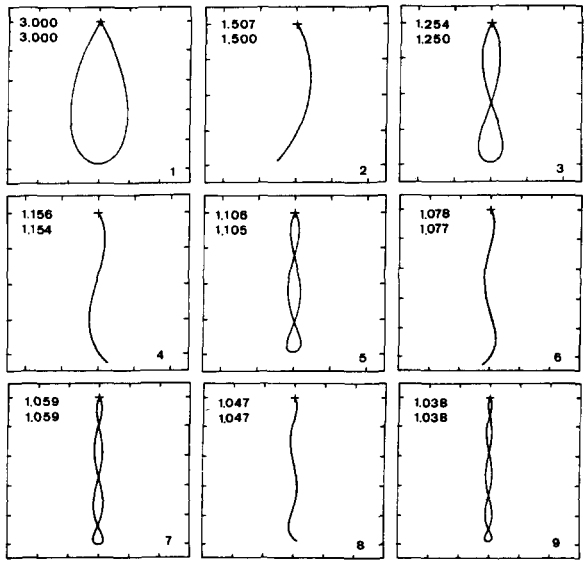


Fig. 10. Small-angle terminating trajectories. The top number on the left is the computer-determined value of the mass ratio ($\mu$). The number underneath is the "magic mass" formula prediction [Eq. (36)]; the value of $N$ is given in the lower right corner of each graph. In each case the swinging mass was launched from the center with a starting angle $\theta_0 = 0.5$ rad; the initial velocity $\dot{r}_0$ varies.

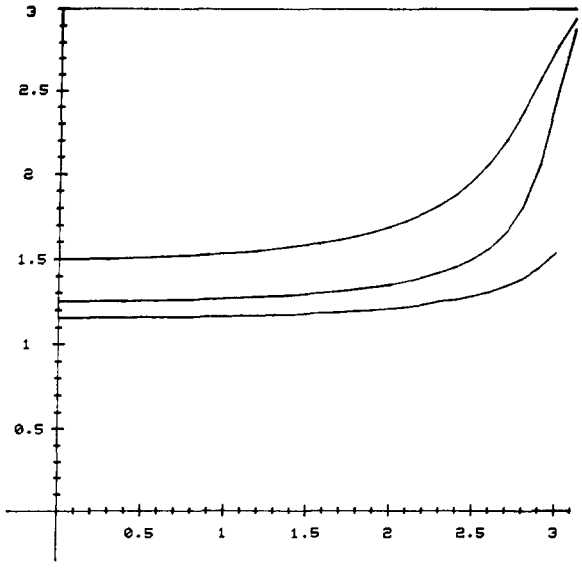


Fig. 11. Mass ratios for simple terminating orbits. The values in Table II are presented graphically. The vertical axis gives the mass ratio ($\mu$); the horizontal axis is the starting angle ($\theta_0$) in radians. The top line, at $\mu = 3$, is for type B1; the next graph down is type B2; next comes type B3; and the bottom graph is type B4.

Even for so large an angle, the agreement with the magic mass formula is remarkably good. Nevertheless, Eq. (36) was derived using a small-angle approximation, and we must expect departures from it when $\theta_0$ is increased. Table II lists computer values of $\mu$ for type B1 ($N = 1$), type B2 ($N = 2$), type B3 ($N = 3$), and type B4 ($N = 4$), as $\theta_0$ ranges from 0.1–3.1 rad. These values are plotted in Fig. 11.

The numerical data reveal a striking and most unexpected feature: for Type B1, the magic mass is independent of the starting angle. *If $\mu = 3$, m will execute one symmetrical loop and return to the pulley, no matter what the launch angle* (or the speed). You may recall that this is not the first time $\mu = 3$ has come into the story: this was also the limiting mass ratio for type A trajectories which begin at $\theta_0 \approx 180°$. Indeed, in this limit the type B1 solution is nothing but a type A trajectory with two extra vertical pieces, and the argument of Sec. IV, paragraph 3, will serve us again to explain why $\mu \to 3$ as $\theta_0 \to \pi$. But it is still a puzzle why $\mu = 3$ for all angles in between.

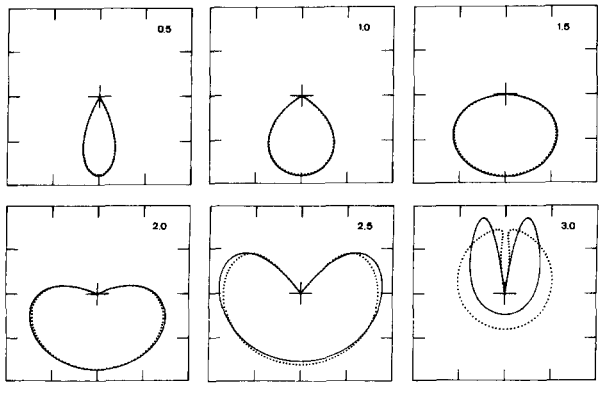


Fig. 12. Perturbative type B1 trajectories. These graphs compare the exact (computer-generated) type B1 solutions (solid lines) with the fifth-order perturbation theory (dotted lines), as given by Eqs. (37) and (38). In each case the swinging mass was launched from the center, the initial velocity of $\dot{r}_0$ varies; the starting angles ($\theta_0$) are given in the upper right corner, in radians.

The perturbation series for type B1 can of course be carried to higher order in $\theta_0$, much as we did for type A in Sec. IV. We shall not present the details, but merely quote the answer, correct to order $\theta_0^5$:

$$r(t) = (4v^2/g)w\left[1 - \tfrac{1}{4}\theta_0^2\, w - \tfrac{1}{8}\theta_0^4 w(w - \tfrac{1}{6})\right], \tag{37}$$

$$\theta(t) = \theta_0 w'\left[1 + \tfrac{1}{3}\theta_0^2 w + \tfrac{1}{5}\theta_0^4 w(w - \tfrac{1}{12})\right], \tag{38}$$

where

$$w = z(1 - z), \quad w' = 1 - 2z, \quad z = gt/4v. \tag{39}$$

Notice that the time it takes to complete the orbit [$\tau = 4v/g$, consistent with Eq. (32), since $\mu = 3$ here] is—like $\mu$—independent of $\theta_0$. Figure 12 shows a comparison between the numerical solutions and perturbation approximation. As expected, the agreement is excellent for small angles, but not so good for $\theta_0$ above $\pi/2$.

## VI. CONCLUSION

The Swinging Atwood's Machine exhibits a variety of interesting kinds of motion, of which we have studied only a few. This is a rich system, and much remains to be done. For instance, there are the higher-order terminating trajectories and higher-order periodic orbits (loops of varying complexity). Among the nonsingular trajectories, we have considered only those which start from rest, and we have said nothing at all about nonbounded motion ($\mu \leqslant 1$). Moreover, as a simple nonlinear system with two degrees of freedom, it may be illuminating to apply to SAM the powerful but abstract ideas developed by Poincaré and Birkhoff[6] and more recent authors.

## ACKNOWLEDGMENT

We wish to thank Richard E. Crandall for many useful suggestions, and for his encouragement and interest in this work.

## APPENDIX

*Theorem*: If $M > m$ then SAM's motion is bounded [$r(t) \leqslant r_{\max}$ for $t \geqslant 0$]. Conversely, if the motion is bounded and nonterminating [$0 < r(t) \leqslant r_{\max}$ for $t > 0$] then $M > m$ (with the trivial exception of stationary balance at $m = M$).

*Proof*: (*a*) *Suppose $M > m$.* Conservation of energy limits the height to which $M$ can rise, and therefore puts an upper bound on $r$. Specifically [using Eq. (10)]:

$$E = \tfrac{1}{2}M\dot{r}^2 + \tfrac{1}{2}m(\dot{r}^2 + r^2\dot{\theta}) + gr(M - m\cos\theta)$$

$$\geqslant gr(M - m\cos\theta) \geqslant gr(M - m).$$

This is *always* true. Now, if $M > m$, it follows that

$$r \leqslant E/g(M - m),$$

so the motion is bounded.

(*b*) *Suppose the motion is bounded and nonterminating.* The essential idea is this: looking at $M$, the average tension in the string ($F$) must balance $Mg$ (for bounded motion); looking at $m$, the average *vertical component* of the tension must balance $mg$. Thus

$$\langle F \rangle = Mg \text{ while } \langle F\cos\theta \rangle = mg. \tag{A1}$$

Since $\cos\theta \leqslant 1$, it follows that $m \leqslant M$ (and if $m = M$ we must have $\theta = 0$ with the system at rest). To prove Eqs. (A1)

formally, define the average of a quantity $q(t)$ in the natural way:

$$\langle q\rangle = \lim_{\tau\to\infty} \frac{1}{\tau}\int_0^\tau q(t)dt. \tag{A2}$$

The tension in the string is given by

$$F = M(g + \ddot{r}). \tag{A3}$$

For bounded motion the average acceleration of $M$ is zero, $\langle \ddot{r}\rangle = 0$, and therefore

$$\langle F\rangle = Mg.$$

Meanwhile, letting $y = r\cos\theta$, we have

$$\ddot{y} = \ddot{r}\cos\theta - 2\dot{r}\dot{\theta}\sin\theta - r\ddot{\theta}\sin\theta - r\dot{\theta}^2\cos\theta. \tag{A4}$$

Using the angular equation (8) to eliminate $\ddot{\theta}$:

$$\ddot{y} = \ddot{r}\cos\theta - r\dot{\theta}^2\cos\theta + g\sin^2\theta,$$

whereupon [applying the radial equation (9)]:

$$m\ddot{y} = mg - F\cos\theta. \tag{A5}$$

For bounded motion, $\langle \ddot{y}\rangle = 0$, and hence

$$\langle F\cos\theta\rangle = mg.$$

[a] Present address: Department of Physics, Boston University, Boston, MA.


[1] E. Breitenberger and R. D. Mueller, J. Math. Phys. **22**, 6 (1981); T. E. Cayton, Am. J. Phys. **45**, 723 (1977); L. Falk, Am. J. Phys. **46**, 1120 (1978); M. G. Rusbridge, Am. J. Phys. **48**, 146 (1980); A. H. Nayfeh and D. T. Mook, *Nonlinear Oscillations* (Wiley, New York, 1979), p. 369.


[2] The transformation $\{r,\theta,t\}\to\{k^2r,\theta,kt\}$ carries solutions to the equations of motion into new solutions, for any constant $k$, so the trajectories scale in $r$. In each graph the scale used is indicated by the ticks along the margins. Thus in Figs. 3 and 4 we have chosen $r_0 = 1$. We used $g = 10$ throughout this study.

[3] Type A occurs when $m$, released from rest, first crosses the vertical axis with purely horizontal velocity (i.e., $\dot{r} = 0$ when $\theta = 0$). If $\mu$ is a little too large the crossing will occur with $\dot{r} < 0$; if $\mu$ is too small, $\dot{r} > 0$. This observation can be developed into a rigorous proof for the existence of type A solutions (Nicholas Tufillaro, senior thesis, Reed College, 1983).

[4] See footnote 2.

[5] $\theta(t)$ is in fact a Gegenbauer Polynomial of index 1 in the variable $(1 - at/v)$: $\theta(t) = G_N^1(1 - at/v)$. See F. W. Byron and R. W. Fuller, *Mathematics of Classical and Quantum Physics* (Addison–Wesley, Reading, MA, 1969), Vol. I, Chap. 5.

[6] See, for example, V. I. Arnold, *Mathematical Methods of Classical Mechanics* (Springer-Verlag, New York, 1978); or G. D. Birkhoff, "Surface Transformations and their Dynamical Applications," in *Collected Mathematical Papers* (Dover, New York, 1966), Vol. 2.

# Instability in automobile braking


W. G. Unruh[a]

*Department of Physics, University of British Columbia, Vancouver, B.C., Canada V6T 2A6*



(Received 1 May 1981; accepted for publication 21 November 1983)



It is shown that the simplest theory for the behavior of automobile tires under braking leads to an instability which causes the car to spin around in cars whose rear wheels lock before the front.


## I. INTRODUCTION

While driving on icy Winnipeg streets in my youth, I would often notice cars spinning around when they braked. Similarly, cars are often seen spinning around when braking hard in trying to avoid an accident. Yet my V.W. Bug was disconcertingly stable while skidding on ice. The suddenness and the short timescale ($\sim$ a few seconds) of the spin in the former cases, and complete absence of spinning in the latter led me to suspect that there was an inherent instability in some cars under hard braking.

In presenting the theory which I believe explains this phenomenon, I would like to begin by posing a problem. The brakes on my car have failed and I can fix either the front or the rear brakes. Which set of brakes should I fix if I am concerned with stability against spinning while braking? I have asked a large number of physicists this question, and the answer almost invariably is "the rear brakes." The reasoning seems to be as follows: When the rear wheels are locked, there will be a friction force between the rear tires and the road directed opposite to the direction of motion of the car (see Fig. 1). If the car rotates, this friction force will apply a torque about the center of mass which tends to straighten out the car. The image they have seems to be that applying the rear brakes is like pulling on the rear of the car with a rope. Since pulling is known to be much more stable than pushing, rear brakes should be more stable than the front brakes. This reasoning is wrong because it neglects the friction forces which act on the front wheels if the car is pointing in a direction which differs from its velocity direction. The front tires can roll only about one axis, i.e., about the wheel axle. If the car has a component of velocity along the axle, the tire must be slipping sideways. Since the surface of the tire is slipping, the full frictional force will develop between the tire and the road. Furthermore, this friction will be directed parallel to the axle. Since this force is perpendicular to the centerline of the car and is of the same order of magnitude as the friction force on the rear wheel, its torque about the center of mass will be much larger than that of the rear wheels. This torque is furthermore of such a sense as to increase the deviation angle between the car's pointing direction and the velocity vector, producing an instability.[1]

If, on the other hand, the front wheels are locked and the rear wheels are free, the role of front and rear wheels in the above argument is interchanged. The larger torque is now exerted by the friction force on the side slipping rear wheels. Now, however, this torque is such as to bring the